International Journal of Astronomy and Astrophysics, 2012, 2, 39-51
http://dx.doi.org/10.4236/ijaa.2012.21007 Published Online March 2012 (http://www.SciRP.org/journal/ijaa)

Surface Photometry and Dynamical Properties of Lenticular Galaxies: NGC3245 as Case Study

Mohamed Adel Sharaf[1], K. Mahmoud[2], E. Aly[3], A. A. Alshaery[4]
[1]Astronomy Department, Faculty of Science, King Abdul Aziz University, Jeddah, Saudi Arabia
[2]Astronomy, Space Science, Meteorology Department, Faculty of Science, Cairo University, Giza, Egypt
[3]Physics Department, National Research Center, Giza, Egypt
[4]Mathematics Department, College of Science for Girls, King Abdul Aziz University, Jeddah, Saudi Arabia
Email: khadiga@sci.cu.edu.eg

Received January 17, 2012; revised February 18, 2012; accepted February 28, 2012

ABSTRACT

In this paper, surface photometry and dynamical properties of Lenticular galaxies will be developed and applied to NGC3245. In this respect, we established new relation between the intensity distribution I and the semi-major axis a Moreover, some basic statistics of both independent and the dependent variables of the relation are also given. In addition to the I(a) relation , the Sérsic $r^{1/n}$ model is applied for the intensity profile I(r) resulting in an estimation of the effective radius, r_e, and the surface brightness it encloses, μ_e. Both relations (I(a) and I(r)) are accurate as judged by the precision criteria which are: the probable errors for the coefficients , the estimated variance of the fit and the Q value (the square distance between the exact solution and the least square estimated solution) where all very satisfactory. Correlation coefficients between some parameters of the isophotes are also computed. Finally as examples of applications of surface photometry we determined the dynamical properties: mass, density, potential distributions, as well as distributions of escape and circular speeds in terms of Sérsic model.

Keywords: Surface Photometry; Dynamical Galaxies

1. Introduction

Surface photometry is a bidimensional broadband technique to quantitatively describe the light distribution of extended objects like galaxies and HII regions. It is a technique rather than a distinct field of research. Reynolds [1] was the first one to try applying surface photometry on galaxies so it is considered as one of the oldest techniques in modern astronomy [2].

Surface photometry is extremely important since it helps us to get information on galactic colors and its implied ages and metallicity gradients [3], stellar populations [4-7], dust content and its extinction [5,8-11], and structure, formation and evolution of galaxies [12,13].

Surface photometry is usually based on fitting ellipses to the isophotes of galaxies especially for ellipticals and lenticulars whose their isophotes show little deviation from being perfect ellipses. Several software packages and tools can perform surface photometry; among them are GALPHOT [14], GASPHOT [15], GALFIT [16], GIM2D [17], and ISOPHOTE.

The package that concerns us here is the ISOPHOTE. The ISOPHOTE's principle task is the ELLIPSE task which does the essential role of fitting the elliptical isophotes to the galaxy image. In addition to ELLIPSE, ISOPHOTE includes some "parameter set" tasks that control the process of ELLIPSE execution and other tasks that test the ELLIPSE performance by examining its results. The algorithm upon which ELLIPSE is based and how to deal with the various tasks is well described in [18] and [19]. The result of applying ELLIPSE task is a table containing the variation of many important quantities, like intensity, ellipse shape parameters, and Fourier coefficients which quantify the amount by which isophotes deviate from perfect ellipses, with semi-major axis. The most important parameter, on which we are interested here, is the intensity distribution. The first goal of this paper, is the establishment of a new relation to describe the intensity profile I(a), in contrast to the usual trials of describing I(r).

On the other hand, intensity profile I(r) plays an important role in finding the distributions density, mass, and potential which play a key role in the understanding of the galactic dynamics. We will derive these dynamical properties in terms of intensity profile I(r), which is the second goal of this paper. This is done by fitting it by a suitable model. A number of models have been put to describe the relation I(r), easily obtained from I(a), the most accepted ones are the Sérsic model for bulges and the exponential law for disks.

In the present paper, we applied the surface photometry on the *g*-band image of the galaxy NGC 3245 obtained from the Sloan Digital Sky Survey (SDSS). The resulted data are shown in Appendix B. Its intensity profile is well fitted by the Sérsic model at n = 2.9, then , we Substituted by Sérsic formula in our derivations for dynamical properties.

NGC 3245 (UGC 5663) is a late S01 galaxy. It is composed of an extremely bright, mildly active nucleus surrounded by a lower-surface brightness (but still very bright), smooth lens ending with a diffuse, faint outer envelope. The nucleus is spherical while both the lens and the envelope have an E5-like flattened structure [20-22]. Jian Hu [23] suggested the coexistence of a central classical bulge and outer boxy bulge in this galaxy since he found it as a boxy one with bulge Sérsic index ~4. Using measurements of surface brightness fluctuations, Tonry *i* [24] determined its distance modulus as 31.6 ± 0.20 (a distance of 20.9 Mpc) [25].

Section 2 describes the basic formulations including the linear least-square modeling of data and some basic statistics. Section 3 presents the new relation for I(a). Section 4 gives a brief description on the Sérsic model and the results of fitting. In Section 5, we derive in detail various dynamical quantities in terms of I(r). The conclusion is given in Section 6. Finally, statistical analysis of ELLIPSE output data is shown in Appendix A.

2. Basic Formulations

2.1. Linear Model Analysis of Observational Data in the Sense of Least-Squares Criterion

Let *z* be represented by the general linear model of the form $\sum_{i=1}^{n} c_i\ \varphi_i(x)$ where φ's are linearly independent functions of x. Let **c** be the vector of the exact values of the c's coefficients and $\hat{\mathbf{c}}$ the least-squares estimators of **c** obtained from the solution of the normal equations of the form $\mathbf{G}\hat{\mathbf{c}} = \mathbf{b}$. The coefficient matrix $\mathbf{G}(n \times n)$ is symmetric positive definite ,that is , all its eigen values λ_i; $i = 1,2,\cdots,n$ are positive. Let $E(f)$ denotes the expectation of f and σ^2 the variance of the fit, defined as:

$$\sigma^2 = \frac{q_n}{N - n} \tag{1}$$

where

$$q_n = \left(\mathbf{y} - \Phi^T\hat{\mathbf{c}}\right)^T\left(\mathbf{y} - \Phi^T\hat{\mathbf{c}}\right), \tag{2}$$

N is the number of observations, **y** is the vector with elements z_k and $\Phi(n \times N)$ has elements $\Phi_{ik} = \Phi_i(x_k)$. The transpose of a vector or a matrix is indicated by the superscript "T". According to the least-squares criterion, it could be shown that [26]

1) The estimators $\hat{\mathbf{c}}$ by the method of least-squares gives the minimum of q_n.

2) The estimators $\hat{\mathbf{c}}$ of the parameters **c**, obtained by the method of least-squares are unbiased; *i.e.* $E(\hat{\mathbf{c}}) = \mathbf{c}$.

3) The variance–covariance matrix $\mathrm{Var}(\hat{\mathbf{c}})$ of the unbiased estimators $\hat{\mathbf{c}}$ is given by:

$$\mathrm{Var}(\hat{\mathbf{c}}) = \sigma^2\mathbf{G}^{-1} \tag{3}$$

4) The average squared distance between $\hat{\mathbf{c}}$ and **c** is:

$$E(L^2) = \sigma^2\sum_{i=1}^{n}\frac{1}{\lambda_i} \tag{4}$$

Finally it should be noted that if the precision is measured by the probable error ν then

$$\nu = 0.6745\ \sigma \tag{5}$$

2.2. Coefficient of Correlation

A coefficient of correlation is a statistical measure of the degree to which two variables x and y (say) are related to each other. In case of a linear equation, the coefficient of correlation is (e.g. [27])

$$R = \frac{N\sum xy - \left(\sum x\right)\left(\sum y\right)}{\sqrt{N\sum x^2 - \left(\sum x\right)^2} \times \sqrt{N\sum y^2 - \left(\sum y\right)^2}} \tag{6}$$

where

$$-1 \le R \le 1$$

$R = \pm 1$ indicates that the two variables are totally correlated, R = 0, no relationship between them, and $|R| \prec 1$ indicates that there is a trend between the two variables x and y. The sign of R indicates whether y is increasing or decreasing when x increasing, while its magnitude indicates how well the linear approximation is.

2.3. Some Basic Statistics

For data analysis of the present paper we used some basic statistics of these are:

1) Descriptive statistic; 2) Location Statistics; 3) Dispersion statistics; 4) Shape statistics.

2.4. Autocorrelation

Autocorrelation is important in time series analysis. Let ρ_k be the autocorrelation at lag k. An estimate of ρ_k is [28]:

$$\rho_k = \sum_{t=1}^{N-k}\left(x_t - \bar{m}\right)\left(x_{t+k} - \bar{m}\right) \Big/ \sum_{t=1}^{N}\left(x_t - \bar{m}\right)^2 \tag{7}$$

where $\bar{m}$ is the mean of the data $x_1, x_2, \cdots, x_N$.

3. New Relation between I and a of the Lenticular Galaxy NGC3245

In what follows, new relation describing the intensity profile along the semi-major axis, I(a) for the lenticular galaxy NGC3245 will be established in the sense of least–squares criterion of Section 2.1. The data used for this relation are the first two columns of **Table I** of Appendix B resulted by applying the IRAF ELLIPSE task on the SDSS *g*-band image of the galaxy.

Moreover, some basic statistics of independent variable (a) and the dependent variable (I) of this relation are given in Appendix A.

The relation and its error analysis are:

3.1. The Fitted Equation

$\mathrm{Log}\, I(a) = c_1 + c_2\, a^{0.44}$.

3.2. The c's Coefficients and Their Probable Errors

$c_1 = 4.05848 \pm 0.00774046$

$c_2 = -0.290529 \pm 0.000867829$.

3.3. The Probable Error of the Fit

$\nu = 0.0403227$.

3.4. The Average Squared Distance between c and $\hat{c}$

$Q = 0.000133351$.

3.5. The Observed and Computed Data

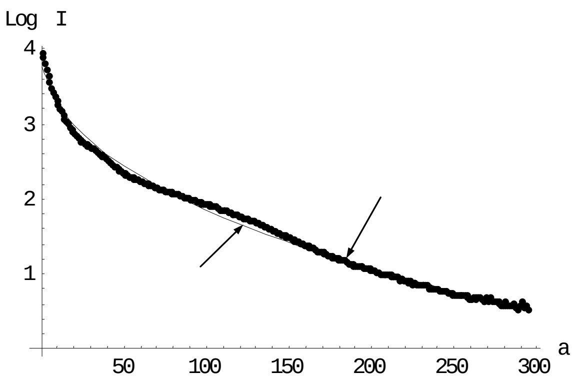

4. Sérsic Model

The intensity distribution along the equivalent radius can be expressed by Sérsic model [29,30]

$$I(r) = I_e e^{-b_n\left[\left(\frac{r}{r_e}\right)^{1/n} - 1\right]}$$

where r_e is the effective radius, the radius encloses half of the whole of the galaxy, I_e is the intensity at this radius, and b_n can be given by the expression

$$b_n = 2n - \frac{1}{3} + \frac{4}{405n} + \frac{46}{25515n^2} + O(n^{-3}), n > 0.36.$$

Detailed deduction and approximation of b_n is discussed in Graham & Driver [31] ([32]).

Starting by the above expression of I(r), Caon *et al.* [33] converted Sérsic's equation to the following formula that describes the surface brightness distribution

$$\mu(r) = \mu_e + \frac{2.5\, b_n}{\ln(10)}\left[\left(\frac{r}{r_e}\right)^{1/n} - 1\right]$$

by using the formula

$$\mu(r) = -2.5 \log I(r)$$

hence, by definition, μ_e is the surface brightness at r_e.

By fitting the intensity profile of the SDSS g-band image of NGC3245 by Sérsic model we found that the profile is well fitted at n = 2.9.

Using the first three columns of **Table I** of Appendix B with $r = a(1-e)$ we get for fitting the intensity profile I(r) by Sérsic model in the sense of least-squares criterion of Section 2.1. the following:

4.1. The Fitted Equation

$\mathrm{Log}\, I(r) = c_1 + c_2\, r^{1/n}$.

4.2. The c's Coefficients and Their Probable Errors

$c_1 = 10.5735 \pm 0.0175424$

$c_2 = 1.44112 \pm 0.00353699$.

4.3. The Probable Error of the Fit

$\nu = 0.0763589$

4.4. The Average Squared Distance between c and $\hat{c}$

$Q = 0.000703915$

4.5. The Observed and Computed Data

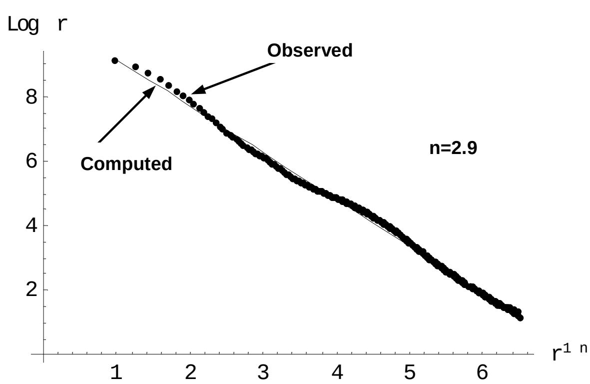

From the values of c_1 and c_2, we get the effective radius $r_e = 18.95''$, whereas $\mu_e = 17.5578$ mag/arcsec^2.

5. Dynamical Properties

The dynamical properties of galaxies can be easily obtained if the intensity profile along radius I(r) is available. As I(r) is the main output from the surface photometry technique, distributions of properties like density, mass, potential, escape and circular velocities can be found as follows:

5.1. Density Distribution

The density distribution is given by

$$\rho(r) = \gamma I(r)$$

where γ is the mass to light ratio.

Sérsic defined I(r) as

$$I(r) = I_e e^{-b_n\left[\left(r/r_e\right)^{1/n}-1\right]}$$

If we defined $k = b_n/r_e^{1/n}$ and $A = e^{bn}$, Sérsic equation can be written as

$$I(r) = I_e A\, e^{-k r^{1/n}}$$

Then, ρ(r) can be written as

$$\rho(r) = \gamma I_e A e^{-k r^{1/n}}$$

5.2. Mass Distribution

The mass enclosed by a given radius r is

$$M(r) = 4\pi\int_0^r \rho(r')r'^2\,dr' .$$

Substituting by the formula of ρ(r)

$$M(r) = 4\pi\gamma I_e A\int_0^r e^{-kr'^{1/n}} r'^2\,dr' .$$

Putting $r'^{1/n} = R, r' = R^n$, and $dr' = nR^{n-1}dR$, then M(r) becomes

$$M(r) = 4\pi n\gamma I_e A\int_0^R e^{-kR}R^{3n-1}dR .$$

Let us consider the general integral

$$Q_m = \int_0^R e^{-kR}R^m\,dR .$$

Integrating, by parts, we get.

$$Q_m = \frac{1}{k}\left(-R^m e^{-kR} + m\,Q_{m-1}\right)$$

Substituting for Q_0, Q_1, Q_2 $\cdots$, we can deduce the relation

$$Q_m = \sum_{j=0}^{m}\frac{m!}{k^{j+1}(m-j)!}R^{m-j}e^{-kR},$$

going back to the initial values of R and m, the final mass descriptive equation is resulted.

$$M(r) = 4\pi n\gamma I_e A\sum_{j=0}^{3n-1}\frac{(3n-1)!}{k^{j+1}(3n-1-j)!}\,r^{3n-1-j}e^{-kr^{1/n}} .$$

If n is a positive fraction , then we have to consider $n = [n]+1$ where [t] is the greatest integer $\le t$ (for our case n is taken as 3).

5.3. Distribution of Potential

The potential in terms of ρ(r) is given by

$$\varphi(r) = -4\pi G\left[\frac{1}{r}\int_0^r \rho(r')r'^2\,dr' + \int_r^\infty \rho(r')r'dr'\right]$$

where G is the gravitational constant. $\varphi(r)$ can be regarded as

$$\varphi(r) = \varphi_1(r) + \varphi_2(r)$$

where

$$\varphi_1 = \frac{-GM(r)}{r},$$

$$\varphi_2 = -4\pi n G\gamma I_e A\int_r^\infty e^{-Kr'^{1/n}}r'dr'$$

by following similar integration steps as that done for mass, φ_2 (r) equals

$$\varphi_2(r) = -4\pi n\gamma G I_e A\sum_{j=0}^{2n-1}\frac{(2n-1)!}{k^{j+1}(2n-1-j)!}\,r^{\frac{2n-1-j}{n}}e^{-kr^{1/n}},$$

substituting by both expressions of φ_1 and φ_2, the final equation of $\varphi(r)$ is

$$\varphi(r) = -G\left[\frac{M(r)}{r} + 4\pi n\gamma I_e A\sum_{j=0}^{2n-1}\frac{(2n-1)!}{k^{j+1}(2n-1-j)!}\,r^{\frac{2n-1-j}{n}}e^{-kr^{1/n}}\right]$$

5.4. Distribution of Escape Speed

The escape speed $v_e(r)$ is given by

$$v_e(r) = \sqrt{2|\varphi(r)|},$$

substitution by $\varphi(r)$ results in

$$v_e(r) = \left[2G\left(\frac{M(r)}{r} + 4\pi n\gamma I_e A\sum_{j=0}^{2n-1}\frac{(2n-1)!}{k^{j+1}(2n-1-j)!}r^{\frac{2n-1-j}{n}}e^{-kr^{1/n}}\right)\right]^{\frac{1}{2}}$$

5.5. Distribution of Circular Speed

$$v_{Cir}^2(r) = r\frac{d\varphi}{dr}$$

by substituting for the expression of $\varphi(r)$ and differentiation, we get

$$v_{Cir}^{2}(r)=\frac{GM(r)}{r}$$
$$-4\pi nG\gamma I_e\left\{\sum_{j=0}^{3n-1}\frac{(3n-1)!}{k^{j+1}(3n-1-j)!}\left[\frac{-k}{n}r^{2n-j}+\frac{3n-1-j}{n}r^{\frac{2n-1-j}{n}}\right]\right.$$
$$\left.+\sum_{j=0}^{2n-1}\frac{(2n-1)!}{k^{j+1}(2n-1-j)!}\left[\frac{-k}{n}r^{\frac{3n-1-j}{n}}+\frac{2n-1-j}{n}r^{\frac{2n-1-j}{n}}\right]\right\}$$

6. Conclusions

In this paper, surface photometry is applied on the lenticular galaxy NGC 3245 as a case study to resulting in the new relation Log I(a) = $c_1 + c_2\, a^{0.44}$, we hope to generalize this relation in the future by applying a large descriptive sample of galaxies.

Since the intensity profile I(r) is well fitted by the Sérsic $r^{1/n}$ model where n = 2.9, we derived relations for various dynamical properties in terms of Sérsic model, strengthening the usefulness of the surface photometry technique.

Both relations, I(a) and I(r), are accurate as judged by a given precision criteria based on linear least-squares fitting criterion. Correlation coefficients between some parameters of the isophotes are also computed.

REFERENCES

[1] R. H. Reynolds, "The Light Curve of the Andromeda Nebula (NGC 224)," *Monthly Notices of the Royal Astronomical Society*, Vol. 74, 1913, pp. 132-136.

[2] S. Okamura, "Surface Photometry of Galaxies," *Publications of the Astronomical Society of the Pacific*, Vol. 100, No. 627, 1988, pp. 524-544. doi:10.1086/132201

[3] H. Wu, Z. Shao, H. J. Mo, X. Xia and Z. Deng, "Optical and Near-Infrared Color Profiles in Nearby Early-Type Galaxies and the Implied Age and Metallicity Gradients," *The Astrophysical Journal*, Vol. 622, No. 1, 2005, pp. 244-259. doi:10.1086/427821

[4] L. Searle, W. L. W. Sargent and W. G. Bagnuolo, "The History of Star Formation and the Colors of Late-Type Galaxies," *The Astrophysical Journal*, Vol. 179, 1973, pp. 427-438. doi:10.1086/151882

[5] R. F. Peletier, E. A. Valentijn, A. F. M. Moorwood and W. Freudling, "The Distribution of Dust in Sb's and Sc's—K-Band Infrared Imaging of a Diameter Limited Sample of 37 Galaxies," *Astronomy and Astrophysics Supplement*, Vol. 108, 1994, pp. 621-641.

[6] D. R. Silva and R. Elston, "Probing Radial Age/Metallicity Degeneracy in Early-Type Galaxies," *The Astrophysical Journal*, Vol. 428, No. 2, 1994, pp. 511-543. doi:10.1086/174263

[7] A. S. Gusev, "Multicolor CCD Photometry of Six Lenticular and Spiral Galaxies. Stellar Population of the Galaxies," *Astronomy Reports*, Vol. 50, No. 3, 2006, pp. 182-193.

[8] R. Evans, "The Variation of the Scalelengths of Galaxies at Different Wavelengths," *Monthly Notices of the Royal Astronomical Society*, Vol. 266, No. 2, 1994, pp. 511-523.

[9] R. F. Peletier, E. A. Valentijn, A. F. M. Moorwood, W. Freudling, J. H. Knapen and J. E. Beckman, "The Extinction by Dust in the Outer Parts of Spiral Galaxies," *Astronomy & Astrophysics*, Vol. 300, No. 1, 1995, p. L1.

[10] R. S. de Jong, "Near-Infrared and Optical Broadband Surface Photometry of 86 face-on Disk Dominated Galaxies. III. The Statistics of the Disk and Bulge Parameters," *Astronomy & Astrophysics*, Vol. 313, 1996, pp. 45-64.

[11] K. Ganda, R. F. Peletier, M. Balcells and J. Falcón-Barroso, "The Nature of Late-Type Spiral Galaxies: Structural Parameters, Optical and Near-Infrared Colour Profiles and Dust Extinction," *Monthly Notices of the Royal Astronomical Society*, Vol. 395, No. 3, 2009, pp. 1669-1694. doi:10.1111/j.1365-2966.2009.14658.x

[12] J. A. L. Aguerri, A. M. Varela, M. Prieto and C. Muñoz-Tuñón, "Optical Surface Photometry of a Sample of Disk Galaxies. I. Observations and Data Reduction," *The Astrophysical Journal*, Vol. 119, No. 4, 2000, pp. 1638-1644.

[13] L. A. M. Tasca and S. D. M .White, "Quantitative Morphology of Galaxies from the SDSS. I. Luminosity in Bulges and Discs," *Astronomy & Astrophysics*, Vol. 530, 2011, p. 106.

[14] W. Freudling, "A Package for Surface Photometry of Galaxies," *Proceedings of 5th ESO/ST-ECF Data Analysis Workshop*, Garching, 26-27 April 1993, p. 27.

[15] E. Pignatelli, G. Fasano and P. Cassata, "GASPHOT: A Tool for Galaxy Automatic Surface PHOTometry," *Astronomy & Astrophysics*, Vol. 446, No. 1, 2006, pp. 373-388.

[16] C. Y. Peng, L. C. Ho, C. D. Impey and H. Rix, "Detailed Structural Decomposition of Galaxy Images," *The Astrophysical Journal*, Vol. 124, No. 1, 2002, pp. 266-293.

[17] F. R. Marleau and L. Simard, "Quantitative Morphology of Galaxies in the Hubble Deep Field," *The Astrophysical Journal*, Vol. 507, No. 2, 1998, pp. 585-600. doi:10.1086/306356

[18] R. I. Jedrzejewski, "CCD Surface Photometry of Elliptical Galaxies. I-Observations, Reduction and Results," *Monthly Notices of the Royal Astronomical Society*, Vol. 226, No. 1, 1987, pp. 747-768.

[19] B. Milvang-Jensen and I. Jørgensen, "Galaxy Surface Photometry," *Baltic Astron*, Vol. 8, 1999, pp. 535-574.

[20] A. Sandage, "The Hubble Atlas of Galaxies," Carnegie Institution of Washington, Washington, 1961.

[21] G. De Vaucouleurs and A. De Vaucouleurs, "Reference Catalogue of Bright Galaxies," University of Texas, Austin, 1964.

[22] A. Sandage and J. Bedke, "The Carnegie Atlas of Galaxies," Vol. I, Carnegie Institution of Washington, Wash-

ington, 1994.

[23] J. Hu, "The Black Hole Mass-Stellar Velocity Dispersion Correlation: Bulges versus Pseudo-Bulges," *Monthly Notices of the Royal Astronomical Society*, Vol. 386, No. 4, 2008, pp. 2242-2252. doi:10.1111/j.1365-2966.2008.13195.x

[24] J. L. Tonry, A. Dressler, J. P. Blakeslee, E. A. Ajhar, A. B. Fletcher, G. A. Luppino, M. R Metzger and C. B. Moore, "The SBF Survey of Galaxy Distances. IV. SBF Magnitudes, Colors, and Distances," *The Astrophysical Journal*, Vol. 546, No. 2, 2001, pp. 681-693. doi:10.1086/318301

[25] A. J. Barth, M. Sarzi, H. Rix, L. C. Ho, A. V. Filippenco and W. W. Sargent, "Evidence for a Supermassive Black Hole in the S0 Galaxy NGC 3245," *The Astrophysical Journal*, Vol. 555, No. 2, 2001, pp. 685-708. doi:10.1086/321523

[26] Z. Kopal and M. A. Sharaf, "Linear Analysis of the Light Curves of Eclipsing Variables," *Astrophysics and Space Science*, Vol. 70, No. 1, 1980, pp. 77-101.

[27] J. Meeus, "Astronomical Algorithms," Willmann-Bell, Inc., Richmond, 2000.

[28] G. E. P. Box and G. M. Jenkins, "Time Series Analysis, Forecasting and Control," Holden-Day, San Francisco, 1976.

[29] J. L. Sérsic, "Atlas de Galaxies Australes," Observatorio Astronomico, Cordoba, 1968.

[30] J. L. Sérsic, "Influence of the Atmospheric and Instrumental Dispersion on the Brightness Distribution in a Galaxy," *Boletin de la Asociacion Argentina de Astronomia*, Vol. 6, 1963, p. 41.

[31] A. W. Graham and S. P. Driver, "A Concise Reference to (Projected) Sérsic $R^{1/n}$ Quantities, Including Concentration, Profile Slopes, Petrosian Indices, and Kron Magnitudes," *Publications of the Astronomical Society of Australia*, Vol. 22, No. 2, 2005, pp. 118-127. doi:10.1071/AS05001

[32] F. Jiang, S. Huang and Q. Gu, "Surface Photometry and Radial Color Gradients of Nearby Luminous Early-Type Galaxies in SDSS Stripe 82," *Research in Astronomy and Astrophysics*, Vol. 11, No. 3, 2011, pp. 309-326.

[33] N. Caon, M. Capacciolo and M. D'Onofrio, "On the Shape of the Light Profiles of Early Type Galaxies," *Monthly Notices of the Royal Astronomical Society*, Vol. 265, No. 4, 1993, p. 1013.

Appendix A

Analysis of the Semi-Major Axis a and the Intensity I of the Lenticular Galaxy NGC3245

I-Coefficients of correlation between ellipse task parameters

Correlation coefficient between a & I= –0.430894

Correlation coefficient between a & e= 0.201083

Correlation coefficient between a & P_a = –0.240178

Correlation coefficient between a & e = –0.81832

Correlation coefficient between a & P_a = 0.860549

Correlation coefficient between a & P_a = –0.662681

II-Statistics of the semi-major axis a

II-1-Basic Descriptive Statistics

- The mean = 148
- The median (central value) = 148
- The variance = 7276.67

II-2-Location Statistics

- The geometric mean = 109.9175238162870485
- The harmonic mean = 47.0803
- The root mean square = 170.751

II-3-Dispersion Statistics

- The Variance of sample mean = 24.6667
- The standard error of sample mean = 4.96655
- The coefficient of variation = 0.576374
- The mean deviation = 73.7492
- The median deviation = 74
- Sample range = 294

II-4-Shape Statistics

- Skewness = 0
- The Pearson skewness 2 = 0
- The kurtosis = 1.79997
- The kurtosis excess = –1.20003

III-Statistics of the intensity I

III-1-Basic descriptive statistics

- The mean = 269.584
- The median (central value) = 31.7
- The Variance = 842620

III-2-Location Statistics

- The Geometric mean = 38.8341456925116324
- The harmonic mean 13.3765
- The root mean square = 955.217

III-3-Dispersion statistics

- The variation of sample mean = 2856.34
- The standard error of sample mean = 53.4447
- The coefficient of variation = 3.40503
- The mean variation = 375.968
- The median variation 27.12
- Sample range = 8644.82

III-4-Shape statistics

- Skewness = 6.23942
- The Pearson skewness 2 = 0.777447
- The kurtosos = 46.9564
- The kurtosos excess = 43.9564

IV-Antocorrelation of the semi-major axis

V-Autocorrelation of the intensity

Table 1. Autocorrelation of the semi-major axis.

k	ρk	k	ρk	k	ρk	k	ρk
0	1	61	0.397339	122	–0.0992227	183	–0.383587
5	0.949162	66	0.31206	127	–0.131955	188	–0.394222
10	0.898382	71	0.305844	132	–0.163203	193	–0.402659
15	0.847719	76	0.261311	137	–0.192908	198	–0.408841
20	0.797232	81	0.217667	142	–0.221013	203	–0.709412
25	0.746978	86	0.174969	147	–0.247458	208	–0.414204
30	0.697016	91	0.133277	152	–0.272185	213	–0.41327
35	0.647405	96	0.0926473	157	–0.295136	218	–0.409846
40	0.598203	101	0.0531398	162	–0.316252	223	–0.403874
45	0.549469	106	0.0148125	167	–0.335475	228	–0.395297
50	0.50126	111	–0.022276	172	–0.352747	233	–0.384055
55	0.453635	116	–0.0580674	177	–0.368009	238	–0.37009
60	0.406653	121	–0.0925933	182	–0.381202	243	–0.353344

k	ρk
244	–0.349656
249	–0.349296
254	–0.306426
259	–0.280387
264	–0.251322
269	–0.219172
274	–0.183879
279	–0.145383
284	–0.103627
289	–0.0585526
294	–0.0101008

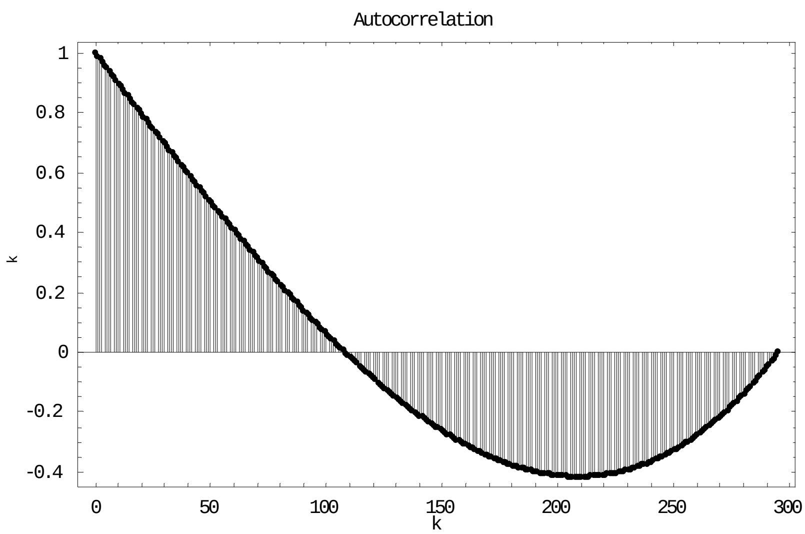

Where ρ_k be the autocorrelation at the lag k.

Table 2. Autocorrelation of the intensity.

k	ρ_k	k	ρ_k	k	ρ_k	k	ρ_k
0	1.	61	0.0125471	122	–0.0246142	183	–0.0474297
5	0.441885	66	0.0083699	127	–0.026959	188	–0.0487461
10	0.245792	71	0.00464442	132	–0.0293067	193	–0.0499393
15	0.155706	76	0.00126099	137	–0.0316098	198	–0.0511356
20	0.111878	81	–0.00206778	142	–0.0337144	203	–0.0522734
25	0.0883066	86	–0.00522823	147	–0.0357281	208	–0.0533318
30	0.0713713	91	–0.00823088	152	–0.0376733	213	–0.0543431
35	0.0562395	96	0.0111305	157	–0.0394688	218	–0.0553028
40	0.0421513	101	–0.0138366	162	–0.0411809	223	–0.0561869
45	0.0313069	106	–0.0166022	167	–0.0427993	228	–0.056985
50	0.0238026	111	–0.0191189	172	–0.0443547	233	–0.0577078
55	0.0182078	116	–0.0216543	177	–0.0457752	238	–0.0583197
60	0.0134611	121	–0.0241443	182	–0.0471521	243	–0.0588403

k	ρ_k
244	–0.0589233
249	–0.0592187
254	–0.0592089
259	–0.0588486
264	–0.058067
269	–0.0569024
274	–0.0551946
279	–0.0522782
284	–0.046794
289	–0.0357456
294	–0.00900998

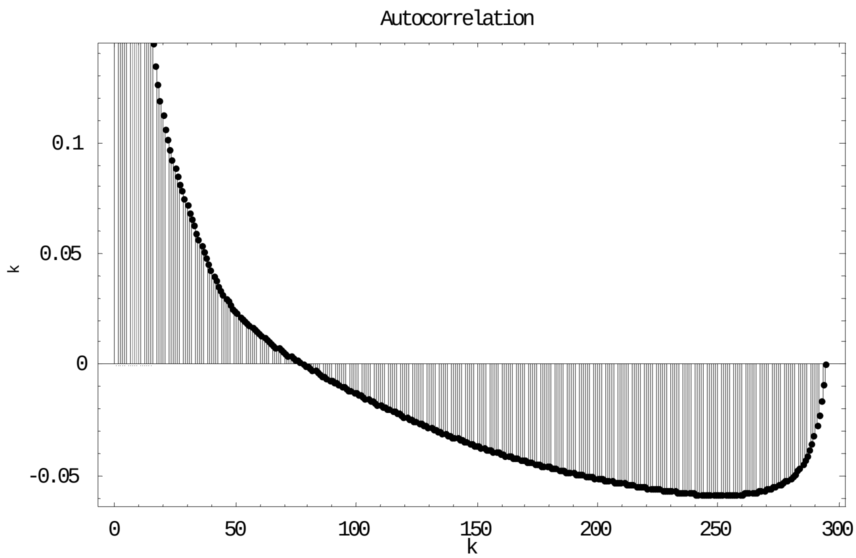

Where ρ_k be the autocorrelation at the lag k.

Appendix B

Table I. Data resulted by ELLIPSE task. Shows the Detailed Distribution of the Intensity I, ellipticity e, and Position angle P.A. along the semi-major axis a, as resulted by The IRAF ELLIPSE task. Semi-major axis is described by pixels where 1 pixel = 0.396″ for the SDSS.

P.A.	e	I (a)	a (pixel)	P.A.	e	I (a)	a (pixel)
–78.23	0.4556	206	52	82.06	0.1101	8648	1
–78	0.4517	199	53	88.84	0.0715	7453	2
–77.84	0.4555	195	54	77.06	0.058	6167	3
–77.9	0.4563	190	55	77.06	0.0414	5030	4
–77.63	0.4575	186	56	83.89	0.0506	4155	5
–77.41	0.4561	181	57	89.14	0.0729	3472	6
–77.44	0.4578	177	58	–85.04	0.1118	2988	7
–77.39	0.4595	174	59	–83.35	0.1415	2590	8
–77.18	0.4604	170	60	–81.97	0.1693	2264	9
–77	0.4589	167	61	–81.45	0.1968	2005	10
–76.62	0.4607	164	62	–81.26	0.216	1783	11
–76.55	0.4577	159	63	–81.08	0.2314	1588	12
–76.96	0.458	156	64	–80.57	0.2435	1419	13
–77.14	0.4545	152	65	–80.56	0.2541	1272	14
–77.1	0.4589	150	66	–80.34	0.2634	1148	15
–77.19	0.4576	147	67	–80.24	0.2741	1047	16
–77.43	0.454	143	68	–80.21	0.2831	960	17
–77.5	0.4553	141	69	–80.07	0.2897	879	18
–77.38	0.4576	139	70	–80	0.2974	809	19
–77.2	0.4587	137	71	–79.82	0.3055	750	20
–77.05	0.4587	133	72	–79.82	0.3186	706	21
–76.89	0.4611	131	73	–80.15	0.3285	663	22
–76.86	0.4601	129	74	–80.08	0.3399	628	23
–77.01	0.4612	127	75	–79.99	0.3492	597	24
–77.1	0.4656	125	76	–79.73	0.3572	567	25
–77.23	0.4686	124	77	–79.57	0.3714	546	26
–77.29	0.4695	122	78	–79.57	0.386	528	27
–77.19	0.4626	118	79	–79.57	0.3996	511	28
–77.23	0.457	116	80	–79.41	0.4106	494	29
–77.21	0.4584	114	81	–79.29	0.4199	477	30
–77.39	0.461	112	82	–79.31	0.4274	461	31
–77.4	0.4637	111	83	–79.34	0.4358	446	32
–77.63	0.4656	109	84	–79.3	0.4443	433	33

Continued

−77.7	0.4692	108	85	−79.24	0.4516	420	34
−77.61	0.4652	106	86	−79.09	0.4573	405	35
−77.96	0.4627	103	87	−78.98	0.4621	391	36
−78.16	0.4624	102	88	−78.98	0.4673	378	37
−78.08	0.4629	100	89	−78.9	0.4718	365	38
−78.08	0.4647	98.5	90	−78.78	0.4708	349	39
−78.1	0.4653	96.3	91	−78.69	0.4695	334	40
−78.56	0.4621	94.9	92	−78.6	0.4684	319	41
−79.04	0.4633	93.8	93	−78.56	0.4669	304	42
−78.88	0.4629	91.8	94	−78.59	0.4663	290	43
−78.66	0.4626	89.6	95	−78.82	0.4647	278	44
−78.89	0.4642	88.6	96	−78.76	0.4591	264	45
−79.21	0.4639	87.3	97	−78.6	0.4573	253	46
−78.92	0.4618	84.8	98	−78.56	0.4587	244	47
−78.92	0.4618	82.7	99	−78.51	0.4576	234	48
−78.92	0.4719	83.3	100	−78.58	0.4603	228	49
−78.76	0.4719	81.6	101	−78.37	0.4572	219	50
−78.71	0.4742	80.5	102	−78.1	0.4544	212	51
−79.28	0.463	26.9	154	−78.6	0.4742	78.9	103
−78.91	0.4599	26.1	155	−78.45	0.4753	77.3	104
−78.95	0.4643	26.1	156	−78.45	0.4793	76.7	105
−78.95	0.4643	25.4	157	−78.61	0.4811	75.4	106
−78.95	0.4643	24.7	158	−78.73	0.4786	73.2	107
−78.77	0.4668	24.3	159	−78.24	0.4757	71.9	108
−78.97	0.4634	23.7	160	−78.45	0.4732	69.9	109
−79.53	0.4634	23.4	161	−78.62	0.4733	68.3	110
−79.53	0.4634	22.6	162	−78.62	0.4768	67.7	111
−78.87	0.4642	22.2	163	−78.83	0.481	67.2	112
−78.87	0.4642	21.7	164	−78.77	0.4835	66.4	113
−79.19	0.4605	21.3	165	−78.71	0.4835	64.8	114
−79.19	0.4535	20.5	166	−78.78	0.4858	64.1	115
−79.57	0.4535	20.1	167	−78.78	0.4825	62.2	116
−78.82	0.4535	19.8	168	−78.59	0.484	61.3	117
−78.82	0.4535	19.2	169	−78.46	0.4863	60.7	118

Continued

–78.99	0.4557	19.1	170	–78.54	0.4855	59.3	119
–78.99	0.4557	18.8	171	–78.95	0.4844	58.2	120
–78.99	0.4557	18.5	172	–78.93	0.4829	56.7	121
–79.92	0.4456	17.5	173	–78.96	0.4822	55.4	122
–78.74	0.4456	17.3	174	–78.87	0.4818	54.3	123
–78.74	0.4456	16.8	175	–78.68	0.4826	53.6	124
–78.74	0.4456	16.4	176	–78.68	0.4837	52.8	125
–79.34	0.4486	16.3	177	–78.81	0.4842	51.8	126
–79.34	0.4486	16	178	–78.87	0.4821	50.4	127
–79.34	0.4486	15.8	179	–78.65	0.4836	49.6	128
–79.74	0.4468	15.5	180	–78.63	0.4858	48.9	129
–79.74	0.4468	15.3	181	–78.64	0.4868	48.1	130
–79.74	0.4468	15.1	182	–78.95	0.4825	47	131
–79.74	0.4468	14.9	183	–78.91	0.4831	46.1	132
–78.98	0.4468	14.7	184	–78.87	0.4835	45.1	133
–78.98	0.4468	14.2	185	–78.87	0.4829	44	134
–78.98	0.4468	13.7	186	–78.91	0.4834	42.8	135
–79.92	0.4354	13.4	187	–78.87	0.4854	42.1	136
–79.92	0.4354	13	188	–78.79	0.4812	40.7	137
–79.19	0.4364	12.9	189	–78.79	0.4796	39.6	138
–79.19	0.4277	12.3	190	–78.96	0.4786	38.6	139
–79.19	0.4391	12.6	191	–78.98	0.48	38	140
–78.84	0.4344	12.3	192	–78.92	0.4732	36.3	141
–79.35	0.4465	12.5	193	–78.92	0.4766	35.9	142
–79.22	0.4465	12.2	194	–78.91	0.4767	35.1	143
–78.5	0.4465	12.1	195	–78.96	0.477	34.7	144
–78.5	0.4465	11.9	196	–78.96	0.477	33.9	145
–78.5	0.4362	11.7	197	–78.96	0.477	32.9	146
–78.5	0.4362	11.5	198	–78.96	0.4763	32	147
–78.87	0.4362	11.4	199	–79.15	0.4762	31.7	148
–78.87	0.4362	11.1	200	–79.3	0.4748	30.8	149
–78.87	0.4362	10.8	201	–79.35	0.4716	29.9	150
–78.87	0.4362	10.8	202	–79.38	0.4712	29.3	151
–78.87	0.4362	10.3	203	–79.38	0.4712	28.9	152
–78.87	0.4362	10.4	204	–79.28	0.4712	28	153
–78.45	0.4163	5.17	256	–78.87	0.4346	10.1	205

Continued

−78.45	0.4163	5.07	257	−78.87	0.4346	9.84	206
−78.79	0.4172	4.93	258	−78.87	0.4346	9.81	207
−78.79	0.4172	4.81	259	−78.87	0.4341	9.68	208
−77.78	0.3991	4.6	260	−78.87	0.4341	9.37	209
−77.78	0.3991	4.5	261	−79.3	0.4403	9.58	210
−78.99	0.4171	4.77	262	−79.3	0.4403	9.41	211
−78.97	0.4089	4.54	263	−79.3	0.4403	9.4	212
−78.17	0.4216	4.67	264	−79.3	0.4403	9.09	213
−78.17	0.44	4.85	265	−79.89	0.4403	9.04	214
−78.17	0.429	4.75	266	−79.99	0.4443	9	215
−78.17	0.4138	4.58	267	−79.99	0.4443	8.69	216
−77.39	0.4004	4.3	268	−80.14	0.4168	8.29	217
−77.58	0.3926	4.14	269	−80.38	0.4168	8.12	218
−80.18	0.4442	4.89	270	−78.45	0.4232	8.18	219
−79.59	0.3903	4.13	271	−78.45	0.4232	8.05	220
−79.59	0.4044	4.38	272	−78.98	0.4155	8.03	221
−79.59	0.431	4.62	273	−79.86	0.4326	8.04	222
−77.36	0.4269	4.31	274	−78.82	0.4169	7.58	223
−79.57	0.4001	4.1	275	−78.82	0.4203	7.66	224
−81.01	0.4063	4.18	276	−78.98	0.4038	7.15	225
−80.35	0.4055	4.04	277	−78.4	0.4251	7.56	226
−79.45	0.4084	4.28	278	−80.19	0.4138	7.21	227
−76.21	0.3697	3.7	279	−79.74	0.4124	7.15	228
−76.94	0.384	3.79	280	−79.74	0.4124	6.9	229
−78.58	0.3752	3.58	281	−79.45	0.4188	7.1	230
−77.87	0.4075	4.27	282	−78.45	0.4225	6.94	231
−76.39	0.3776	3.58	283	−79.79	0.4234	6.88	232
−78.32	0.3972	3.77	284	−78.04	0.4285	6.87	233
−77.11	0.4029	3.68	285	−79.63	0.4286	6.91	234
−78.07	0.4052	3.83	286	−78.64	0.4075	6.5	235
−76.4	0.3765	3.63	287	−78.34	0.4075	6.3	236
−79.28	0.3765	3.36	288	−78.34	0.4075	6.07	237
−76.94	0.3765	3.35	289	−78.7	0.3999	6.07	238
−79.06	0.4132	3.68	290	−78.7	0.4189	6.3	239

Continued

−79.47	0.4213	3.78	291	−78.7	0.409	6.18	240
−76.55	0.4213	4.11	292	−78.7	0.4142	6.17	241
−80.49	0.4179	3.57	293	−78.45	0.4142	5.92	242
−77.13	0.4179	3.73	294	−78.72	0.4138	5.9	243
−76.49	0.39	3.18	295	−78.72	0.4114	5.73	244
				−78.72	0.4085	5.68	245
				−80.4	0.4113	5.67	246
				−79.02	0.4034	5.42	247
				−77.91	0.4034	5.25	248
				−77.25	0.4214	5.49	249
				−79.21	0.4042	5.15	250
				−79.21	0.4042	5.13	251
				−79.21	0.4146	5.18	252
				−81.1	0.4055	5.08	253
				−78.13	0.3872	4.91	254
				−78.45	0.4163	5.14	255